Surface Densities of High Turbulence Intensity Premixed Flames

G. J. Smallwood, D. R. Snelling, and Ö. L. Gülder

Combustion Research Group, ICPET
National Research Council
1500 Montreal Road, Bldg. M-9
Ottawa, ON K1A 0R6, Canada

greg.smallwood@nrc.ca
dave.snelling@nrc.ca
omer.gulder@nrc.ca

Introduction

The concept of laminar flamelets provides a useful tool to model turbulent premixed combustion using simple assumptions. At high enough Damköhler numbers, it is assumed that the turbulent brush of a premixed flame consists of a region of reactants and products separated by laminar flamelets [1-3]. The mean rate of conversion of reactants into products per unit volume, $\langle w \rangle$, can be expressed as [2]

$$\langle w \rangle = \rho_r\, S_L^o\, I_o\, \Sigma \tag{1}$$

where ρ_r is the density of reactants, S_L^o is the normal laminar burning velocity, I_o is a flamelet stretch and curvature correction term, Σ is the flamelet surface density defined as the mean flame surface area per unit volume, and $\langle\ \rangle$ indicates a mean value.

The Bray-Moss-Libby model (BML) [4] for Σ is based on the spatial distribution of flame crossings along a contour of mean progress variable, $\langle c \rangle$, which is 0 in the reactants and 1 in the products, and is represented algebraically by

$$\Sigma = g/(\sigma y L y) \cdot [\langle c \rangle(1\text{-}\langle c \rangle)] \tag{2}$$

where g is a constant of the order unity, σ_y is a mean direction cosine, and L_y is a characteristic length related to flame wrinkling. An alternative formulation for modeling the spatial variation of the flame surface density, based on the gradient of the progress variable across the flame front [5], is

$$\Sigma = \langle \Sigma' \rangle = \langle \left| \nabla c \right| \cdot \delta(c\text{-}c_f) \rangle \tag{3}$$

where ∇c is the spatial flame front gradient, $\delta(c\text{-}c_f)$ is the instantaneous flame front position, and Σ' is the instantaneous flame surface density.

To determine Σ for a three-dimensional flowfield from two-dimensional images, knowledge of the orientation of the normal to the flame front relative to the image plane is required. To ascertain the orientation, images from orthogonal planes may be used to determine the mean crossing angle along the line of intersection of the planes. The Bunsen flame represents a simplification in that its flowfield is axisymmetric. Assuming that the flame front has a symmetric mean orientation behavior about the axis, the normal to the flame front can be determined without requiring an orthogonal view.

In this study, surface densities of turbulent premixed flames in a Bunsen flame have been evaluated from planar images obtained using laser-induced fluorescence of OH. Flame front statistics of the Bunsen flames are compared and the implications are discussed. The significance of the turbulence intensity in determining the flame surface density is examined over a wide range of u'/S_L.

Table 1. Summary of Experimental Conditions

Data Set	No. of images	U (m/s)	u' (m/s)	Φ	S_L (m/s)	u'/S_L	Λ (mm)	Σ_{max} (mm^{-1})
BY21	800	11	0.36	1.0	0.43	0.84	1.5	0.30
BX91	800	14	0.59	1.0	0.43	1.4	2.3	0.31
BX98	800	14	0.62	0.8	0.30	2.0	2.5	0.30
JL11	800	42	2.78	1.0	0.43	6.47	1.8	0.37
JB11	100	42	2.78	1.0	0.43	6.47	1.8	0.37
JR11	100	42	2.78	1.0	0.43	6.47	1.8	0.31
JC11	100	42	2.73	0.8	0.30	9.10	1.9	0.36
JR12	100	77	4.49	1.0	0.43	10.44	1.6	0.33
JB12	100	77	4.50	0.8	0.30	15.00	1.7	0.31
JB13	100	39	2.28	1.0	0.43	5.30	1.5	0.28
JR18	100	73	3.69	1.0	0.43	8.58	1.8	0.25
JB18	100	72	3.87	0.8	0.30	12.90	1.7	0.22
JR19	100	53	3.05	1.0	0.43	7.09	1.6	0.24
JB19	100	56	3.38	1.0	0.43	7.86	1.6	0.27

Experimental Methodology

An axisymmetric Bunsen-type burner with nozzle diameters of 11.2 mm and 22.4 mm produced the turbulent premixed conical flames studied. The conditions for the Bunsen flames are reported in Table 1. The instantaneous flame fronts were visualized by PLIF (planar laser-induced fluorescence) of the OH radical. A tunable XeCl excimer laser (308 nm) was wavelength tuned to a strong OH molecular resonance line, $Q_1(3)$. The dimensions of the laser sheet at the burner centerline were about 17 cm (vertical) by 100 μm (horizontal), expanding to 150 μm at the radial periphery of the flame.

The images were acquired with an intensified CCD detector (576x384 pixels) equipped with a Nikon 105 mm UV imaging lens with an image spatial resolution of 248 μm. Due to negligible flame radiation, absence of laser scattering, and high OH signal, no image correction was required.

Setting a threshold of 60 after scaling the images from 0 to 255 systematically binarized the images. Pixel values of 1 indicate a progress variable equal to 1 (burnt gases) and pixel values of 0 indicate a progress variable of 0 (fresh mixture). The resulting image represents the instantaneous map of the progress variable. By averaging over the number of images selected (100 to 800) one determines the mean progress variable map. Individual flame contours (1 pixel wide) were detected from the instantaneous maps of the fresh/burnt gases, as can be seen in Fig. 1. As the apparatus did not permit simultaneous acquisition of orthogonal images, we assumed

$$\Sigma = \left\langle \Sigma' \right\rangle = \left\langle \frac{\Sigma'_{xy}}{\cos\theta_{xz}} \right\rangle \approx \frac{\left\langle \Sigma'_{xy} \right\rangle}{\left\langle \cos\theta_{xz} \right\rangle} \approx \frac{\left\langle \Sigma'_{xy} \right\rangle}{\cos\left\langle \theta_{xz} \right\rangle} \tag{4}$$

which should be valid for moderate turbulence intensities. $\Sigma_{xy} = \langle \Sigma'_{xy} \rangle = \langle |\nabla c_i|_{xy} \cdot \delta_{xy}(c-c_f) \rangle$ and $\langle \theta_{xz} \rangle$ were then determined over the number of images. As the Bunsen flame is axisymmetric, Σ was obtained by dividing $\langle \Sigma'_{xy} \rangle$ by $cos\langle \theta_{xy} \rangle$, which must be statistically equal to $cos\langle \theta_{xz} \rangle$ along the axis of the burner, assuming isotropic turbulence.

Results and Discussion and Conclusions

The Σ profile, including individual data points, for one representative Bunsen flame is shown on Fig. 2 as a function of $\langle c \rangle$. This shows data averaged from 100 flame images. Increasing the number of images, as shown in Fig. 3, can reduce the scatter in the data. This shows data averaged from 800 flame images for another representative Bunsen flame. The solid lines in Figs. 2 and 3 represent a Lowess smooth of the data. The mean two-dimensional flame surface density, Σ_{xy}, and the mean orientation angle which produced the Σ profiles were also determined. The Σ_{xy} profiles are symmetric about $\langle c \rangle$=0.5. The mean direction cosines ($\cos\langle \theta \rangle$) of the flame front had a typical value of

0.69 for all the Bunsen flames. This is in good agreement with the typical value of 0.7 found in numerous experimental studies [6-8] and computed by DNS [9].

The profiles in Figs. 2 and 3 are typical of those found for the other flames. They are also typical of those found at low to moderate turbulence intensities (u'/S_L = 0.25 to 2.0) in Bunsen flames and spark ignition engines [6,7]. The profiles determined in this study are comparable in shape to those found by Veynante et al. [10] in a two-dimensional V-flame and by Deschamps et al. [11] in a Bunsen flame but under different turbulence conditions.

Σ_{max} has little variation over the range of u'/S_L (0.8 to 15.0) investigated here, as can be seen in Fig. 4. Clearly, there is no relationship between flame surface density and turbulence intensity. It has been shown that $\Sigma \cdot \Lambda$ increases with increasing u'/S_L at low turbulence intensities [8]. However, this is likely due to the contribution from the integral length scale, which also varied in the reported experiments. This relation is shown for our wider range of turbulence intensities in Fig. 5, where it can be seen that there is no obvious relationship between $\Sigma \cdot \Lambda$ and u'/S_L. In fact, it has already been shown that the flame surface density has a strong inverse relationship with the integral length scale [6,7], when normalized by the laminar flame thickness.

The observation that the surface density (as well as its maximum value) does not change with the nondimensional turbulence intensity (Fig. 4) has some serious implications. Experimental observations on turbulent premixed flames have shown that $\langle w \rangle$ (or turbulent burning velocity) increases with increasing turbulence. Thus the flame surface density is expected to increase with increasing u'/S_L in accordance with Eq. 1. However, the flame surface density shows no evidence of dependence on the flow turbulence (see Table 1). If the surface density is a true measure of the characteristics of the wrinkled flame surface, then Eq. 1 may not be a reasonable assumption for the flamelet regime, and the turbulent premixed combustion analysis and predictions should not be based only on the geometry of the flame front surface.

References

1. Bray, K. N. C., in Complex Chemical Reactive Systems, (J. Warnatz and W. Jäger, Eds.), Springer-Verlag, 1987, pp. 356-375.
2. Cant, R. S., and Bray, K. N. C., Twenty-Second Symposium (International) on Combustion, The Combustion Institute, Pittsburgh, 1986, pp. 791-799.
3. Peters, N., Twenty-First Symposium (International) on Combustion, The Combustion Institute, Pittsburgh, 1986, pp. 1231-1250.
4. Bray, K. N. C., Libby, P. A., and Moss, B. J., Combust. Sci. Tech. 41:143-172 (1984).
5. Pope, S. B., Int. J. Engng. Sci. 26:445-469 (1988).
6. Deschamps, B. M., Smallwood, G. J., Prieur, J., Snelling, D. R., and Gülder, Ö. L., Twenty-Sixth Symposium (International) on Combustion, The Combustion Institute, Pittsburgh, 1996, pp. 427-435.
7. Smallwood, G. J. and Deschamps, B. M., SAE Paper No. 962088 (1996).
8. Ghenaï, C., Chauveau, C., and Gökalp, I., Twenty-Sixth Symposium (International) on Combustion, The Combustion Institute, Pittsburgh, 1996, pp. 331-337.
9. Trouvé, A. and Poinsot, T., J. Fluid Mech., 278:1-31 (1994).
10. Veynante, D., Duclos, J. M., Piana, J., Twenty-Fifth Symposium (International) on Combustion, The Combustion Institute, Pittsburgh, 1994, pp. 1249-1256.
11. Deschamps, B., Boukhalfa, A., Chauveau, C., Gökalp, I., Shepherd, I. G., and Cheng, R. K., Twenty-Fourth Symposium (International) on Combustion, The Combustion Institute, Pittsburgh, 1992, pp. 469-475.

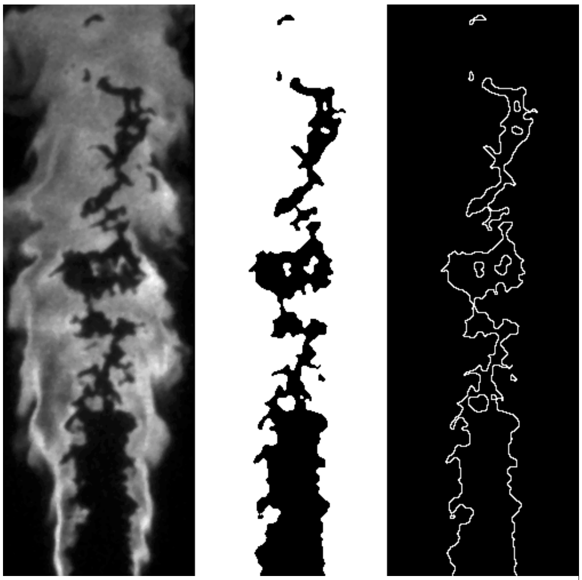

Fig. 1. Sample flame OH image, binary image, and edge image, for u'/S_L = 15.00.

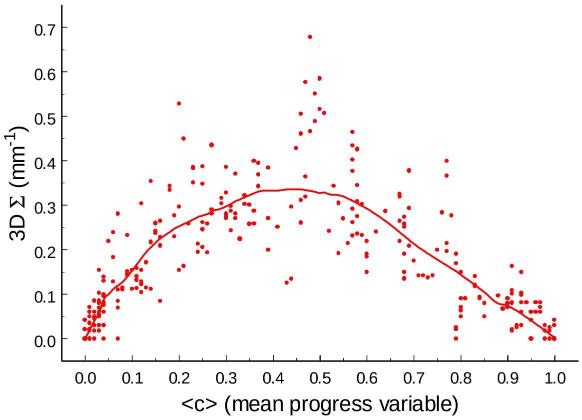

Fig. 2. Flame surface density as a function of mean progress variable, for u'/S_L = 10.44 (100 images).

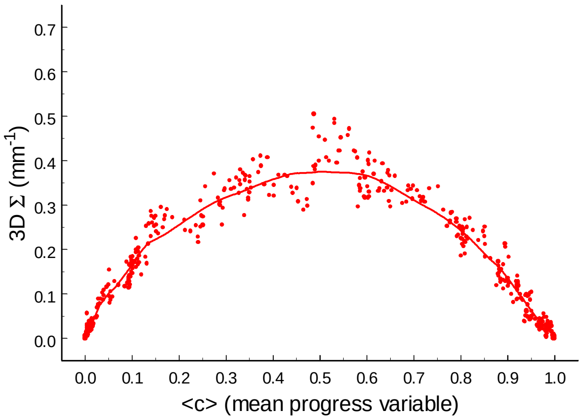

Fig. 3. Flame surface density as a function of mean progress variable, for u'/S_L = 6.47 (800 images).

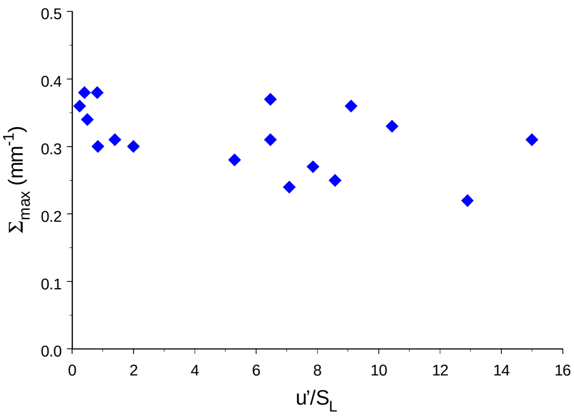

Fig. 4. Maximum flame surface density versus nondimensional turbulence intensity in premixed propane/air flames.

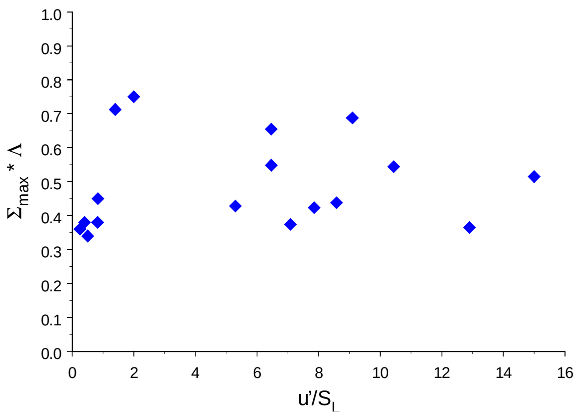

Fig. 5. Maximum flame surface density normalized by the integral length scale versus nondimensional turbulence intensity in premixed propane/air flames.